Integrative *In Vitro* and *In Silico* Analysis Reveals Multi-Targeted Anticancer Effects of Berberine Chloride on Breast Cancer

Abir Salek
abirsalek18@gmail.com
University of Monastir
Mouna Selmi
University of Monastir
Aida Lahmer
University of Monastir
Mabrouk Horchani
University of Monastir
Mouna Maatouk
University of Monastir
Mahassen Barboura
University of Monastir
Haifa Messai
University of Monastir
Jihed Boubabaker
University of Monastir
Hichem Ben Jannet
University of Monastir
Leila Chekir-Ghedira
University of Monastir
Ines Bouhlel-Chatti
University of Monastir

Article

Keywords: Berberine chloride, breast cancer, cell viability, apoptosis, metastasis, Molecular docking

Posted Date: January 28th, 2026

DOI: https://doi.org/10.21203/rs.3.rs-8567883/v1

Additional Declarations: No competing interests reported.

Abstract

Berberine chloride (BRB), an isoquinoline alkaloid isolated from *Berberis vulgaris*, demonstrated significant anticancer activity against breast cancer. This study assessed the therapeutic effects of BRB on cell proliferation, cell cycle progression, apoptosis, and metastasis in human (MDA-MB-231) and murine (4T1) triple-negative breast cancer cells. Cytotoxicity testing with a crystal violet assay showed an IC_{50} of 40 µM for MDA-MB-231 and 10 µM for 4T1 after 48 hours of treatment. BRB induced S-phase cell cycle arrest in MDA-MB-231 and G2/M phase arrest in 4T1 cells. It also induced late apoptosis in both cell lines, along with increased reactive oxygen species production and loss of mitochondrial membrane potential. Furthermore, BRB exhibited anti-angiogenic effects by inhibiting cell migration, as demonstrated by scratch wound and Transwell assays. Additionally, BRB reduced adhesion to various extracellular matrix components, with the most noticeable effect seen with collagen IV in both cell lines. Molecular docking simulations indicated that BRB has a favorable binding energy with multiple cancer-related targets, including MDM2-P53, BCL2, Caspases (3, 8, and 9), MCL1 complexes, and matrix metalloproteinases (MMP-2 and MMP-9). The compound maintained stable hydrogen bonds, ππ-stacking interactions, and hydrophobic contacts, often achieving higher docking scores than the co-crystallized ligand. Overall, the results suggest that BRB exerts multi-targeted anticancer effects by regulating processes such as proliferation, apoptosis, migration, and adhesion, indicating that BRB could be a promising candidate for breast cancer therapy.

Introduction

Breast cancer remains the most common cancer among women worldwide. It is the leading cause of cancer death in women and the third overall cause of cancer-related mortality (1). It accounts for approximately 25% of all cancer diagnoses and causes 15% of all cancer deaths in women. Despite advances in early detection and multimodal treatments including surgery, chemotherapy, radiotherapy, and hormone therapy, breast cancer continues to be a significant public health concern (2). Recent progress in genetic and molecular profiling has revealed the extensive heterogeneity of breast cancer, complicating prognosis and treatment. Among its many subtypes, triple-negative breast cancer (TNBC) is particularly aggressive, lacking hormone receptors and HER2 receptors, and is highly prone to early metastatic recurrence (3). Chemotherapy remains the primary treatment for TNBC, but is often limited by dose-related toxicity to healthy tissues and a high rate of drug resistance. These factors significantly contribute to mortality from breast cancer and underscore the urgent need for new therapeutic strategies (2). Many natural compounds found in food, known as phytochemicals, are increasingly being used in the prevention and treatment of breast cancer due to their potential pharmacological properties. Phytochemicals are plant-based molecules that have been used for centuries in traditional medicine and are now being studied for their potential as anticancer agents and as supplements to conventional therapies. This study investigates the antitumor effects of berberine chloride (BRB), a naturally occurring isoquinoline alkaloid from *Berberis vulgaris*, due to its diverse biological activities, including antibacterial (4, 5), antidiabetic (6, 7), anti-inflammatory (8), and anticancer effects (9–11). Additionally, molecular docking simulations were performed to explore the binding affinities and potential inhibitory interactions of BRB with key molecular targets associated with cancer. These computational analyses aimed to uncover possible mechanisms behind its observed biological effects. The docking results showed favorable interactions of BRB with various proteins involved in tumor growth, apoptosis, and metastasis, such as MDM2–P53, BCL2, caspases, MCL1 complexes, and matrix metalloproteinases (MMPs). These in silico findings provide a solid structural basis for the experimental results and support BRB's potential as a multi-target anticancer agent(12–14).

Materials and Methods

Cell Lines and Cell Culture

Human and murine breast cancer cell lines, MDA-MB-231 and 4T1, respectively, were obtained from the American Type Culture Collection (ATCC, Molsheim, France). Cells were cultured in Dulbecco's Modified Eagle Medium (DMEM) (PAN Biotech, Tunisia) supplemented with 10% fetal bovine serum (FBS) (PAN Biotech, Tunisia) and 100 U/mL of L-glutamine and penicillin-streptomycin (PAN Biotech, Tunisia). Cells were maintained in a humidified atmosphere at 37°C with 5% CO_2.

1. Cell Viability Assays

Cells were seeded at a density of 5×10^3 cells per well on 96-well plates and allowed to attach for 24 hours. They were then treated with increasing concentrations (0–100 μM) of berberine chloride (BRB), purchased from Alfa Aesar, Thermofisher, Germany, for 48 hours. Cell viability was assessed using the crystal violet assay (Sigma-Aldrich, France) according to the manufacturer's instructions. Cell viability was calculated with GraphPad Prism version 8.0 software (GraphPad Software, San Diego, CA, USA).

2. Cell Cycle Analysis

Cell cycle distribution was analyzed using the FC 500 MPL flow cytometer (BD FACSCanto™ cytometer). Briefly, 2×10^5 cells were seeded per well in a 6-well plate and treated with the following concentrations of BRB ($½\times IC_{50}$, IC_{50}, and $1.5\times IC_{50}$) for 48 hours. Afterwards, cells were washed with PBS and stained for 1 hour at 37°C with a solution containing 200 μg/mL RNase A and 50 μg/mL PI (Sigma-Aldrich, France). At the end of the incubation, cells were washed with cold PBS, and PI fluorescence, which varies according to DNA content and cell cycle phase, was measured and analyzed with FlowJo software v.10 (Tree Star, Ashland, OR, USA).

3. Apoptosis Analysis

Cell viability was assessed by flow cytometry using Annexin V-PI. Briefly, 2×10^5 cells were seeded per well in a 6-well plate and treated with the following concentrations of BRB ($½\times IC_{50}$, IC_{50}, and $1.5\times IC_{50}$) for 48 hours. Both floating and adherent cells were stained with 5 μL of Annexin V-FITC and 5 μL of PI in 50 μL of binding buffer for 15 minutes at room temperature in the dark. Afterwards, 200 μL of binding buffer was added, and the cells were analyzed using a BD FACSCanto™ cytometer.

4. Intracellular ROS Accumulation

The intracellular ROS level was measured using a nonfluorescent probe, 2,7-diacetyl dichlorofluorescein (DCFH-DA), which penetrates the cell's interior where it is oxidized by ROS to form fluorescent dichlorofluorescein (DCF). MDA-MB-231 and 4T1 cells were incubated with ($½\times IC_{50}$, IC_{50}, and $1.5\times IC_{50}$ of BRB) for 48 hours. Then, 5 μL of a 25 μM solution of 2,7-dichlorofluorescein diacetate (DCFH-DA; Fluka, Steinheim, Germany) was added to each well. After 1 hour of incubation, the fluorescence in each well was measured every 5 minutes for 1 hour using a fluorescence microplate reader (Biotek, Winooski, VT, USA) with a 538 nm emission and a 485 nm excitation filter. The area under the fluorescence versus time curve was integrated at each time point to compute the ROS units. The median effective dose (IC50) was determined from the median effect plot of log (fa/fu) versus log (dose), where fa is the fraction affected and fu is the fraction unaffected by the treatment.

5. Mitochondrial Membrane Potential (ΔYm) analysis

The effect of BRB on mitochondrial membrane potential was measured using rhodamine 123 (Sigma Aldrich). Briefly, treated cells were harvested, washed twice with PBS, and then incubated at 37°C for 20 minutes with a staining buffer containing rhodamine 123. Fluorescence intensity was detected using a fluorescence microplate reader (BioTek, Winooski, VT, USA) with 595 nm emission and 488 nm excitation filters.

6. Effect on Cell Adhesion

To investigate how BRB affects metastasis in breast cancer (BC) cells, we first tested its ability to change cell adhesion in the presence of three main extracellular matrix (ECM) components. Research shows that an ECM rich in type I collagen can give untransformed cells a tumor-like phenotype. Likewise, fibronectin is known to induce epithelial-mesenchymal transition (EMT) in BC cells and plays a key role in helping metastasis. In this study, we examined how BRB influences BC cell adhesion to

collagen type I, collagen type IV, and fibronectin, three factors that increase during EMT. Briefly, a 96-well flat-bottom microtiter plate (Nunc) was coated with 50 µL of a protein solution containing fibronectin, collagen types I and IV at 10 µg/mL, and poly-L-lysine at 50 µg/mL for 2 hours at 37°C. Next, the wells were saturated with 50 µL of PBS/BSA 0.5% for 1 hour at the same temperature. Cells were then detached from culture flasks using PBS/EDTA (0.1%), rinsed twice with adhesion buffer, and pre-incubated with different concentrations of BRB (½×IC_{50}, IC_{50}, and 1.5×IC_{50}) for 30 minutes at room temperature with gentle agitation. Subsequently, 50 µL of a cell suspension containing 1×10^6 cells/mL in adhesion buffer was added to each well and incubated for 1 hour at 37°C. After incubation, non-adherent cells were removed by rinsing with adhesion buffer. The adherent cells were fixed with 1% glutaraldehyde for 10 minutes at room temperature, rinsed twice with distilled water, and stained for 30 minutes with 0.1% crystal violet. After washing, the dye was solubilized using 100 µL of 1% sodium dodecyl sulfate (SDS), and cell adhesion was measured by reading the absorbance at 600 nm.

7. Cell migration

7.1. Wound Healing Assay

Cells were seeded at a density of 2 × 10^6 cells per well in 6-well plates. Once the cells reached approximately 90% confluence, they were scratched with a sterile pipette tip, and any floating cells and debris were removed by washing with complete medium. The cells were then treated with different concentrations of BRB (½×IC_{50}, IC_{50}, and 1.5×IC_{50}) for 48 hours. Images of the plates were taken at three time points: T = 0 (immediately after scratching), T = 24 hours, and T = 48 hours. The scratch area was analyzed using ImageJ software. Cell migration was measured as the percentage of surface recovery using the following formula:

% Recovery = [(AT0 − AT24/48) / AT0] × 100

7.2. Transwell Cell Migration

The transwell insert is a technique used to measure cell migration, consisting of an upper chamber and a lower chamber separated by a polycarbonate membrane with 8 µm diameter pores. The upper compartment contains a cell suspension, while the lower compartment contains a chemotactic substance, allowing cells to migrate through the membrane to the lower chamber. The membrane is pre-coated with collagen IV at 10 µg/mL in PBS overnight at 4°C, and the lower chamber is filled with migration buffer (DMEM/BSA 0.1%). Cells are detached from culture flasks using PBS/EDTA (0.1%), rinsed twice with adhesion buffer, and pre-incubated with different concentrations of BRB (½×IC_{50}, IC_{50}, and 1.5×IC_{50}) for 30 minutes at room temperature with gentle agitation before being placed in the upper chamber and incubated for 48 hours at 37°C with 5% CO_2. After incubation, migrated cells on the underside are fixed with 1% glutaraldehyde and stained with 0.1% crystal violet. Excess dye is washed off with distilled water, and migration images are captured using an inverted microscope. Cell migration is quantified by measuring absorbance at 600 nm after solubilizing the dye in 1% sodium dodecyl sulfate (SDS).

8. Molecular docking procedure

Molecular docking simulations were performed *via* the Auto Dock 4.2 program package (15). The crystal structures of: His6-tagged Mdm2 in complex with nutlin-3a (pdb: 5ZXF), BCL-2 with venetoclax (pdb: 6O0K), caspase-3 (apopain or cpp32) in complex with an isatin sulfonamide inhibitor (pdb: 1GFW), procaspase-8 in complex with covalent small molecule inhibitor 63-R (pdb: 6PX9), dimeric caspase-9 (pdb: 2AR9), Mcl-1 in complex with the BaxBH3 (pdb: 3PK1), Mcl-1 bound to BID-MM domain (pdb: 5C3F), catalytic domain of mmp-2 complexed with sc-74020 (pdb: 1HOV), hydroxamate based inhibitor EN140 in complex with the MMP-9 catalytic domain (pdb: 4WZV) were downloaded from the RSCB protein data bank (https://www.rcsb.org/). Initially, water molecules were removed, and missing hydrogen atoms, along with Gasteiger charges, were added during the preparation of the receptor input file. Subsequently, AutoDock Tools were employed to prepare the ligands and protein files in PDBQT format. The optimization of all the geometries of compounds was performed by ACD (3D viewer) software (http://www.filefacts.com/acd3d-viewer-freeware-info), and the visualization and analysis of interactions were performed using

Discovery Studio 2017R2 (https://www.3dsbiovia.com/products/collaborative-science/biovia-discovery-studio/) and PyMOL 0.99rc6(16).

Statistical Analyses

Data are presented as mean ± standard error of the mean (SEM), as specified in the figure legends. Statistical analyses were conducted using GraphPad Prism 8.0 software (GraphPad Software, La Jolla, San Diego, CA, USA). Comparisons between groups were performed using one-way and two-way analysis of variance (ANOVA), followed by Dunnett's multiple comparison test. A p-value of ≤ 0.05 was considered statistically significant (*** $p < 0.001$, and **** $p < 0.0001$).

Results

1. BRB Inhibits the Proliferation of Breast Carcinoma Cells

We initially assessed the cytotoxic effects of BRB on triple-negative human breast cancer cell lines, MDA-MB-231, and the murine 4T1 cell line. Using CV cell viability assays, we found that BRB exhibited a dose-dependent cytotoxic effect after 48 hours of treatment with concentrations from 0 to 100 μM (Fig. 1). The calculated inhibitory concentration of 50% (IC50) after this period was 40 μM for MDA-MB-231 and 10 μM for the 4T1 cell line. Based on these values at 48 hours, we selected the following IC50-related doses for subsequent experiments: 0.5-fold IC50 ($0.5 \times IC_{50}$), IC50, and 1.5-fold IC50 ($1.5 \times IC_{50}$).

2. BRB Induces cell cycle arrest of breast Carcinoma Cells

The cell cycle encompasses all biochemical and morphological events that promote cell proliferation. This study highlights the impact of berberine (BRB) on the cell cycle and its ability to induce apoptosis in breast cancer cells. Using flow cytometry, the research demonstrated that BRB specifically causes arrest in the S phase of MDA-MB-231 cells, while it affects 4T1 cells differently (Fig. 2A). Additionally, there was a notable decrease in the number of cells in the G0/G1 phase, along with the emergence of a sub-G1 peak. This peak indicates apoptotic cells with reduced DNA content due to fragmentation during apoptosis.

3. BRB induces apoptosis in breast Carcinoma Cells

During apoptosis, phosphatidylserine moves from the inner to the outer leaflet of the plasma membrane, a process that can be visualized using the annexin V/PI double-labeling technique. This method helps distinguish between early and late stages of apoptosis: cells in early apoptosis are only labeled with annexin V, while those in late apoptosis show both annexin V and PI labeling. Recent findings indicate that treating cells with BRB for 48 hours significantly increases the number of cells labeled only with annexin V, indicating a higher proportion of early apoptotic cells. Additionally, there is an increase in cells labeled with both annexin V and PI, suggesting more late apoptotic cells after BRB treatment (Fig. 2B, 2C).

4. BRB induces ROS accumulation in breast Carcinoma Cells

Reactive oxygen species (ROS) are key mediators of apoptosis. To assess ROS production, we measured the oxidation of DCFH to the fluorescent compound DCF following exposure of cells to increasing concentrations of BRB. We found a significant, dose-dependent rise in ROS levels in both cell lines. In MDA-MB-231 cells, ROS levels increased to 180%, 213%, and 234% with 20, 40, and 60 μg/mL BRB, respectively, compared to the control (100%). Conversely, 4T1 cells showed a smaller increase, reaching 112%, 121%, and 154% at 5, 10, and 15 μg/mL BRB, respectively. These findings suggest that BRB induces a greater production of ROS in MDA-MB-231 cells than in 4T1 cells (Fig. 3A).

5. BRB decreases mitochondrial transmembrane potential in breast Carcinoma Cells

Monitoring mitochondrial transmembrane potential (ΔΨm) is a reliable indicator of cell metabolism, apoptosis, and overall viability. The effect of BRB on ΔΨm in the MDA-MB-231 and 4T1 cell lines was assessed using rhodamine 123 staining. BRB treatment for 48 hours significantly decreased ΔΨm in both tumor cell types in a dose-dependent manner, indicating impaired mitochondrial function and increased membrane permeability. In MDA-MB-231 cells, ΔΨm dropped to 86%, 75%, and 64% at 20, 40, and 60 µg/mL of BRB, respectively, compared to untreated control cells (100%). Similarly, in 4T1 cells, ΔΨm decreased to 84%, 78%, and 71% at 5, 10, and 15 µg/mL of BRB, respectively. These findings clearly demonstrate that BRB disrupts mitochondrial membrane potential in a dose-dependent manner.

6. BRB decreases cell adhesion in breast Carcinoma Cells

The ability of cells to adhere to wells coated with different types of ECM was tested one hour after seeding, following a 30-minute treatment with BRB at three concentrations based on previously established IC_{50} values. The results showed that BRB significantly reduced cell adhesion in a dose-dependent manner in both MDA-MB-231 and 4T1 cells. Specifically, cell adhesion to collagen IV was reduced the most, by approximately 40% at the highest BRB concentration tested, while it decreased by 30% on collagen I and 20% on fibronectin. In contrast, cell adhesion to poly-L-lysine, an integrin independent substrate, remained largely unchanged. Therefore, BRB disrupts cell adhesion mainly by interfering with integrin-mediated interactions (Fig. 4).

7. BRB decreases cell migration in breast carcinoma Cells

Cell migration is a key step in cancer metastasis. Two complementary assays were performed to assess the effect of BRB on this process: the wound-healing assay (Fig. 5) and the Boyden chamber (Transwell) assay (Fig. 6).

In the wound-healing assay, the untreated MDA-MB-231 and 4T1 cells fully closed the wound after 48 hours of incubation at 37°C with 5% CO_2. Conversely, BRB significantly inhibited wound closure in a dose- and time-dependent manner. In MDA-MB-231 cells, it reduced migration to 80% at the highest concentration after 24 hours and to 75% after 48 hours. In 4T1 cells, the effect was even more pronounced, decreasing migration to 50% after 24 hours and 40% after 48 hours compared to untreated controls, thereby preventing full wound closure.

In line with these observations, the Boyden chamber assay also showed that BRB significantly decreased the migratory ability of both cell types in a concentration-dependent manner. At the highest concentration of BRB, 48-hour treatment reduced cell migration by approximately 75% in MDA-MB-231 and 80% in 4T1 cells.

8. Molecular Docking Analysis

The combination of computational and experimental methods has proven highly effective in identifying and developing promising new compounds. Widely used in modern drug design, molecular docking techniques analyze the conformations that ligands adopt within the binding sites of macromolecular targets. These methods also estimate the binding free energy between ligands and receptors by examining key factors involved in intermolecular recognition (15). In this context, we performed docking simulations of berberine against several targets. The docking results shown in Table 1 indicate that, in most cases, berberine achieved a more favorable score than the co-crystallized ligand. Furthermore, Fig. 7 presents a 3D model illustrating how well this ligand fits into the binding cavities of all targeted receptors. For additional details, the 2D models in Fig. 8 reveal that berberine forms several noteworthy interactions. Against MDM2-P53, the docked ligand participates in a conventional hydrogen bond with Tyr79, a C-H bond with Gln51, Pi-Sigma interactions with Val72 and His75, Pi-Pi stacking with His75, and Alkyl/Pi-Alkyl interactions with Ile40, Met41, and Val72. With BCL2, berberine forms a C-H bond with Phe112 and several Alkyl/Pi-Alkyl contacts with residues Met115, Leu137, Arg146, Ala149, and Val156. Regarding Caspase 3, berberine engages in a conventional hydrogen bond with Phe252, C-H bonds with Ser205, Arg207, and Ser251, Pi-Sigma interactions with Ser251, Pi-Pi T-shaped interactions with Phe112, and Pi-Alkyl contacts with Trp206. Against Caspase 8, berberine forms an H-bond with Arg258, Pi-Cation interactions with Arg260, Pi-Sigma with Trp420, and Alkyl/Pi-Alkyl contacts with Arg258 and Cys360. For Caspase 9, the ligand shows an H-bond with Arg178, a C-H bond with Gln285, Pi-Cation interactions with Arg180

and Arg355, and an Alkyl interaction with Arg355. Regarding the MCL1-BAX target, berberine forms an H-bond with Arg263, Pi-Sigma interactions with Val249 and Val253, Pi-Sulfur with Met231, Pi-Pi T-shaped interactions with Phe270, and Alkyl/Pi-Alkyl contacts with Met231, Leu235, Val253, Leu267, and Phe270. For MCL1-BID, berberine interacts with Arg263 via a hydrogen bond, forms Pi-Sigma interactions with Val249 and Val253, a Pi-Sulfur interaction with Met231, and a Pi-Pi T-shaped interaction with Phe270. It also engages in Alkyl/Pi-Alkyl contacts with Met231, Leu235, Val253, Leu267, and Phe270. Moving to MMP-2, berberine exhibits an H-bond with Ala84, C-H bonds with Val117, Ala139, and Pro140, Pi-Anion interaction with Glu121, Pi-Sigma with Leu83, Pi-Pi stacking with His120, and Pi-Alkyl interactions with Ala84, Val117, His120, and His130. Against MMP-9, berberine forms an H-bond with Gly186, a C-H bond with Pro246, Pi-Sigma interaction with His226, and Alkyl/Pi-Alkyl contacts with Leu188, Met247, and Met247. Overall, these results clearly demonstrate that berberine tends to inhibit the selected cancer targets.

Table 1
Binding energy of the docked Berberine in the binding cavity of selected receptors.

	apoptotic proteins							**metalloproteinase**	
Targeted receptor	MDM2-P53 (pdb: 5ZXF)	BCL2 (pdb: 6O0K)	Caspase 3 (pdb: 1GFW)	Caspase 8 (pdb: 6PX9)	Caspase 9 (pdb: 2AR9)	MCL1-BAX (pdb: 3PK1)	MCL1-BID (pdb: 5C3F)	MMP-2 (pdb: 1HOV)	MMP-9 (pdb: 4WZV)
Binding Energy (kcal/mol)									
Berberine	-6.9	-7.9	-7.0	-6.6	-5.9	-6.9	-6.7	-7.4	-7.9
Co-crystallized ligand	-6.7	-10	-6.0	-5.7	-4.0	*	*	-5.3	-9
* : The targeted receptor hasn’t a Co-crystallized ligand.									

Discussion

In the present study, it is noteworthy that BRB exhibited strong anti-cancer and anti-metastatic effects against human breast cancer cells, as well as murine MDA-MB-231 and 4T1 cells. Indeed, BRB has a significant inhibitory effect on cell viability by inducing apoptosis, causing cell cycle arrest, generating ROS, disrupting mitochondrial potential, and inhibiting the migration, adhesion, and invasion of cancer cells compared to untreated cells. Cell migration, adhesion, and invasion are essential steps in the metastatic spread of cancer. The current therapeutic approach emphasizes treatments targeting molecules involved in carcinogenesis.

The effect of BRB on cell viability was assessed using the Crystal Violet test. The results showed that BRB has cytotoxic activity against the two studied cell lines, significantly reducing their viability. These findings align with reports from various authors who have demonstrated BRB's notable antiproliferative effects against different types of cancer, including colorectal, prostate, melanoma, and especially breast cancer(17–20). Studies have indicated that BRB inhibits the proliferation of MDA-MB-231 cells in a time and concentration dependent manner(9). Several researchers also confirm the effectiveness of BRB in cancer treatment. Recent *in vitro* studies with cancer cell lines reveal that BBR inhibits cancer cell proliferation and migration and induces apoptosis in various lines (21, 22). It is worth noting that this proliferation inhibition could result from several intracellular processes, such as cell cycle blockage or induction of apoptosis. To verify the cause of the antiproliferative effect, we monitored the cell cycle progression after BRB treatment, using flow cytometry a quick and straightforward method for cell cycle analysis. Results indicated that BRB caused growth arrest in MDA-MB-231 cells at the S phase and in 4T1 cells at the G2/M phase. Control cells showed normal progression through G1, S, and G2/M phases across both lines. This suggests that BRB induces cell cycle arrest in MDA-MB-231 cells at the S phase and in HUVEC cells at the G2/M phase(23–25). It is also reported that BRB's cell cycle arrest effect in human cancer cell lines may involve its interaction with DNA(26). The impact on cell distribution depends on cell type and treatment specifics. For instance, G0/G1 phase arrest has been observed in breast

cancer (like MCF-7 cells) (27), colorectal carcinoma (HCT-8 and HCT-116) (28) (29), and ovarian carcinoma (OVCAR-3 and Skov-3) (30). In giant cell and prostate carcinomas, BBR affects cyclins D1, D2, E, and Cdk2, Cdk4, and Cdk6, leading to G0/G1 arrest and suppressed proliferation (31). Apoptosis displays various morphological, membranous, mitochondrial, and nuclear changes detectable by flow cytometry (32). Annexin V, a calcium-dependent protein with high affinity for phosphatidylserines, combined with propidium iodide (PI), allows early and late apoptosis detection. After 48-hour BRB treatment, there was a significant, dose-dependent increase in annexin V-positive cells, indicating early apoptosis, and an increase in annexin V and PI double-stained cells, reflecting late apoptosis. Since apoptosis involves multiple signaling pathways, we investigated BRB's ability to generate reactive oxygen species (ROS) in both cell lines. We measured ROS production by monitoring DCFH oxidation to fluorescent DCF following BRB treatment. Results revealed a dose-dependent increase in ROS, more pronounced in MDA-MB-231 cells. Elevated ROS can compromise mitochondrial membrane potential, activate apoptotic factors like AIF, and trigger caspase-independent apoptosis (33, 34). Analysis of cytosolic and mitochondrial fractions showed increased cytochrome c levels in the cytosol after 48 hours of BRB treatment, activating caspase-9 and suggesting cytochrome c-dependent apoptosis. Other studies indicate that ROS generation post-BRB treatment activates kinases like JNK and p38, promoting apoptosis. We assessed mitochondrial transmembrane potential (ΔΨm) using rhodamine 123 staining. BRB reduced ΔΨm in a concentration-dependent manner, indicating mitochondrial dysfunction, a key early step in apoptosis. Several research groups have documented BRB's pro-apoptotic effects through mitochondria, showing it disrupts membrane potential, inhibits respiration, and modulates Bcl-2 family member expression (35–37). During metastasis, cancer cells detach from primary tumors, circulate, and invade new tissues, which requires adhesion and migration through the vascular endothelium. Since cell adhesion is vital for extravasation, we evaluated BRB's effect on MDA-MB-231 and 4T1 cell adhesion. Cells were treated with increasing BRB doses and then seeded on wells coated with extracellular matrices like fibronectin, collagen I, collagen IV, laminin, and poly-L-lysine (an adhesion substrate independent of integrins). Results showed BRB inhibited adhesion to fibronectin, collagen I, and notably collagen IV, but did not significantly affect adhesion to poly-L-lysine, implying its action involves integrins. These findings support previous research showing that BRB has strong anti-metastatic potential by reducing cancer cell adhesion to matrix components such as collagen IV and laminin, along with impairing motility. Since cell interaction with the extracellular matrix and soluble factors is crucial for metastasis, we also examined BRB's impact on cell migration through wound healing and Boyden chamber assays. In wound healing, untreated cells completely closed the wound within 48 hours, while BRB-treated cells showed reduced migration, proportional to concentration and time. Boyden chamber results confirmed significant migration inhibition by BRB in both cell lines, in a dose-dependent manner. These results support existing studies demonstrating that BRB can reduce tumor cell migration and metastasis (9)(38–40). Additionally, we studied BRB’s ability to prevent invasion of MDA-MB-231 and 4T1 spheroids through agarose gel, where high concentrations of BRB inhibited invasion by about 80%. Tumor tissue extracellular matrix, mainly collagen, contributes to tumor stiffness and invasion guidance in invasive tumors, with collagen fibers aligned perpendicularly to the tumor boundary(41).The integration of molecular docking with experimental findings provides a deeper look at the detailed mechanisms that account for the anticancer action of BRB. Docking studies showed that BRB has the potential to exert high binding affinities for various cancer-related protein targets, including MDM2–p53, BCL2, Caspases (3, 8, and 9), MCL1–BAX, MCL1–BID, MMP-2, and MMP-9, using various interactions such as hydrogen bonding and π–π stacking and hydrophobic contacts with active-site residues. More importantly, these in silico results are in good agreement with the presented in vitro observations. These predicted bindings of BRB to BCL2 and caspases have thus demonstrated its capacity for activation of the mitochondrial apoptotic pathway through the release of cytochrome c along with the activation of caspase-9. Moreover, the high affinity of BRB against MMP-2 and MMP-9 was found to be in close agreement with its inhibitory effects on cell migration and invasion, suggesting that BRB probably acts by interfering with the breakdown of the extracellular matrix and metastasis. In addition, its predicted interaction with the MDM2–p53 complex suggests that BRB could stabilize or reactivate p53 function, therefore contributing to its antiproliferative and pro-apoptotic properties.

Taken together, our findings show that berberine exerts potent cytotoxic, pro-apoptotic, and anti-metastatic effects in both human and murine breast cancer cells. BRB effectively impairs crucial hallmarks of malignancy through mitochondrial dysfunction, ROS generation, and interference with integrin-mediated adhesion and migration. Molecular docking data support these mechanisms by identifying specific protein targets through which BRB may act to execute its multi-targeted anticancer

actions. These combined experimental and computational results strongly support the therapeutic promise of berberine as a natural anticancer agent and warrant further in vivo and clinical investigations.

Declarations

Conflict of Interest Disclosure

The authors declare no conflicts of interest.

Funding Statement

This research received no external funding.

Author Contribution

Authors' Contributions: A.S and M.S : writing original manuscript, Methodology, Writing – review & editingA.L, M.M, M.B, and J.B : Formal analysis,Software, Conceptualization,H.M: English editing L.C.G : Resources, L.C.G and I.B.C; Supervision and ValidationM.H and H.B.J : molecular docking All authors have read and agreed to the published version of the manuscript.

Acknowledgement

The work was supported by the Tunisian Ministry of Higher Education and Scientific Research (TMHESR).

Data Availability

The datasets generated during the current study are available from the corresponding author.

References

1. Global Cancer Incidence and Mortality Rates and Trends—An. Update | Cancer Epidemiology, Biomarkers & Prevention | American Association for Cancer Research [Internet]. [cited 2025 Sept 19]. Available from: https://aacrjournals.org/cebp/article/25/1/16/157144/Global-Cancer-Incidence-and-Mortality-Rates-and
2. Triple Negative Breast Cancer Treatment Options and Limitations. Future Outlook [Internet]. [cited 2025 Nov 4]. Available from: https://www.mdpi.com/1999-4923/15/7/1796
3. Triple-negative breast. cancer: challenges and opportunities of a heterogeneous disease | Nature Reviews Clinical Oncology [Internet]. [cited 2025 Nov 4]. Available from: https://www.nature.com/articles/nrclinonc.2016.66
4. BJNANO - Antibacterial. activity of a berberine nanoformulation [Internet]. [cited 2025 Nov 4]. Available from: https://www.beilstein-journals.org/bjnano/articles/13/56
5. Wojtyczka, R. D. et al. Berberine Enhances the Antibacterial Activity of Selected Antibiotics against Coagulase-Negative Staphylococcus Strains in Vitro. *Molecules* **19** (5), 6583–6596 (2014).
6. Addressing the preventive and therapeutic perspective of berberine against diabetes. Heliyon [Internet]. [cited 2025 Nov 4]. Available from: https://www.cell.com/heliyon/fulltext/S2405-8440(23)08441-4
7. Berberine and Its Study as. an Antidiabetic Compound [Internet]. [cited 2025 Nov 4]. Available from: https://www.mdpi.com/2079-7737/12/7/973?cid=62785818358&utm_source=organic&utm_campaign=&utm_medium=&utm_content=&utm_term=.

8. Anti-inflammatory potential. of berberine-rich extract via modulation of inflammation biomarkers - Naz – 2022 - Journal of Food Biochemistry - Wiley Online Library [Internet]. [cited 2025 Nov 4]. Available from: https://onlinelibrary.wiley.com/doi/full/10.1111/jfbc.14389
9. Salek, A. et al. Enhancement of the In Vitro Antitumor Effects of Berberine Chloride When Encapsulated within Small Extracellular Vesicles. Pharmaceutics. Sept 9;14(9):1913. (2022).
10. Berberine as a Potential Anticancer Agent. A Comprehensive Review [Internet]. [cited 2025 Nov 4]. Available from: https://www.mdpi.com/1420-3049/26/23/7368
11. Anticancer properties of berberine -. analysis of the latest reports | Journal of Education, Health and Sport [Internet]. [cited 2025 Nov 4]. Available from: https://apcz.umk.pl/JEHS/article/view/48332
12. Hokarne, C. E. B. A. et al. *Dr Balaji Shivraj. Multidisciplinary Research in Arts, Science & Commerce (Volume-15)* 65 (The Hill Publication, 2024).
13. Molecular Docking and Structure-. Based Drug Design Strategies [Internet]. [cited 2025 Nov 4]. Available from: https://www.mdpi.com/1420-3049/20/7/13384
14. Molecular Docking |. SpringerLink [Internet]. [cited 2025 Nov 4]. Available from: https://link.springer.com/protocol/10.1007/978-1-59745-177-2_19
15. AutoDock, V. Improving the speed and accuracy of docking with a new scoring function, efficient optimization, and multithreading - Trott – 2010 - Journal of Computational Chemistry - Wiley Online Library [Internet]. [cited 2025 Nov 4]. Available from: https://onlinelibrary.wiley.com/doi/full/10.1002/jcc.21334
16. The PyMOL molecular. graphics system | CiNii Research [Internet]. [cited 2025 Nov 4]. Available from: https://cir.nii.ac.jp/crid/1370294643858081026
17. Berberine as a Potential Anticancer Agent. A Comprehensive Review [Internet]. [cited 2025 Nov 8]. Available from: https://www.mdpi.com/1420-3049/26/23/7368
18. Xiong, R. G. et al. Anticancer Effects and Mechanisms of Berberine from Medicinal Herbs: An Update Review. *Molecules* **27** (14), 4523 (2022).
19. Almatroodi, S. A., Alsahli, M. A. & Rahmani, A. H. Berberine: An Important Emphasis on Its Anticancer Effects through Modulation of Various Cell Signaling Pathways. *Molecules* **27** (18), 5889 (2022).
20. Liu, D., Meng, X., Wu, D., Qiu, Z. & Luo, H. A. Natural Isoquinoline Alkaloid With Antitumor Activity: Studies of the Biological Activities of Berberine. Front Pharmacol [Internet]. Feb 14 [cited 2025 Nov 8];10. Available from: https://www.frontiersin.org/journals/pharmacology/articles/ (2019). 10.3389/fphar.2019.00009/full
21. Kim, J. B. et al. The alkaloid Berberine inhibits the growth of Anoikis-resistant MCF-7 and MDA-MB-231 breast cancer cell lines by inducing cell cycle arrest. *Phytomedicine* **17** (6), 436–440 (2010).
22. Berberine-induced growth inhibition of epithelial ovarian carcinoma cell lines - Park. – 2012 - Journal of Obstetrics and Gynaecology Research - Wiley Online Library [Internet]. [cited 2025 Nov 8]. (2011). Available from: https://obgyn.onlinelibrary.wiley.com/doi/full/10.1111/j.1447-0756.01743.x?casa_token=_IqonlPDrWwAAAAA%3AV2ph3d5h1LXmuk45ho9NPNvdv_OH4Wfz0XhZiUdB6_OQDfXYo_dSRxkxG_Djaej6mp-0XQ20pSkJqoGe.
23. Induction of G. 1 cell cycle arrest and apoptosis by berberine in bladder cancer cells - ScienceDirect [Internet]. [cited 2025 Nov 8]. Available from: https://www.sciencedirect.com/science/article/abs/pii/S0014299911004110
24. Lin, J. P., Yang, J. S., Lee, J. H., Hsieh, W. T. & Chung, J. G. Berberine induces cell cycle arrest and apoptosis in human gastric carcinoma SNU-5 cell line. *World J. Gastroenterol. WJG.* **12** (1), 21–28 (2006).
25. Li, Q., Zhao, H., Chen, W. & Huang, P. Berberine induces apoptosis and arrests the cell cycle in multiple cancer cell lines. *Arch. Med. Sci. AMS.* **19** (5), 1530–1537 (2021).
26. Berberine inhibits non-small cell lung cancer cell growth through. repressing DNA repair and replication rather than through apoptosis - Ni – 2022 - Clinical and Experimental Pharmacology and Physiology - Wiley Online Library [Internet]. [cited 2025 Nov 8]. Available from: https://onlinelibrary.wiley.com/doi/full/10.1111/1440-1681.13582?

casa_token=PQ33XG6dUvQAAAAA%3AMb6Ouj0U4n2hHUOtftF0HpbAG-w25ljtlTyvsvHHVQ4EljgCeD5jE1WwoBsGUdD3onthUsbfIX4zFx-w

27. Almatroodi, S. A., Alsahli, M. A. & Rahmani, A. H. Berberine: An Important Emphasis on Its Anticancer Effects through Modulation of Various Cell Signaling Pathways. *Molecules* **27** (18), 5889 (2022).
28. Samad, M. A., Saiman, M. Z., Abdul Majid, N., Karsani, S. A. & Yaacob, J. S. Berberine Inhibits Telomerase Activity and Induces Cell Cycle Arrest and Telomere Erosion in Colorectal Cancer Cell Line, HCT 116. *Molecules* **26** (2), 376 (2021).
29. Anvarbatcha, R., Kunnathodi, F. & Islam, M. Induction of G0/G1 phase cell cycle arrest and apoptosis by thymol through ROS generation and caspase-9/-3 activation in breast and colorectal cancer cell lines. *J. Cancer Res. Ther.* **19** (7), 1915 (2023).
30. Umar, T. et al. A REVIEW OF BERBERINE BIOACTIVE COMPOUNDS AND ITS THERAPEUTIC POTENTIAL IN OVARIAN CANCER.
31. Nano Metal Based Herbal Theranostics for Cancer Management. Coalescing Nature's Boon with Nanotechnological Advancement | Bentham Science Publishers [Internet]. [cited 2025 Nov 8]. Available from: https://www.benthamdirect.com/content/journals/cpb/10.2174/1389201022666210122141724
32. Henry, C. M., Hollville, E. & Martin, S. J. Measuring apoptosis by microscopy and flow cytometry. *Methods* **1** (2), 90–97 (2013 June).
33. Zong, L. & Liang, Z. Apoptosis-inducing factor: a mitochondrial protein associated with metabolic diseases—a narrative review. *Cardiovasc. Diagn. Ther. 2023 June* **30**;13(3):609–622 .
34. Apoptosis, A. Comprehensive Overview of Signaling Pathways, Morphological Changes, and Physiological Significance and Therapeutic Implications [Internet]. [cited 2025 Nov 8]. Available from: https://www.mdpi.com/2073-4409/13/22/1838
35. Berberine An Important Emphasis on Its Anticancer Effects through Modulation of Various Cell Signaling Pathways [Internet]. [cited 2025 Nov 8]. Available from: https://www.mdpi.com/1420-3049/27/18/5889
36. Frontiers | Research progress on the pharmacological effects. of berberine targeting mitochondria [Internet]. [cited 2025 Nov 8]. (2022). Available from: https://www.frontiersin.org/journals/endocrinology/articles/10.3389/fendo.982145/full.
37. Frontiers | Apoptosis Induction, a Sharp Edge of Berberine to Exert Anti-Cancer Effects, Focus on Breast, Lung, and Liver Cancer [Internet]. [cited 2025 Nov 8]. Available from: https://www.frontiersin.org/journals/pharmacology/articles/10.3389/fphar.2022.803717/full
38. Berberine Inhibited Growth and Migration of Human Colon Cancer Cell Lines by Increasing. Phosphatase and Tensin and Inhibiting Aquaporins 1, 3 and 5 Expressions [Internet]. [cited 2025 Nov 8]. Available from: https://www.mdpi.com/1420-3049/28/9/3823
39. Yang, L. J. et al. Berberine hydrochloride inhibits migration ability via increasing inducible NO synthase and peroxynitrite in HTR-8/SVneo cells. *J. Ethnopharmacol.* **305**, 116087 (2023).
40. The Core-Targeted RRM2 Gene of Berberine Hydrochloride Promotes Breast Cancer Cell. Migration and Invasion via the Epithelial–Mesenchymal Transition [Internet]. [cited 2025 Nov 8]. Available from: https://www.mdpi.com/1424-8247/16/1/42
41. Elastocapillary effects determine early matrix. deformation by glioblastoma cell spheroids | APL Bioengineering | AIP Publishing [Internet]. [cited 2025 Nov 8]. Available from: https://pubs.aip.org/aip/apb/article/8/2/026109/3289142

Figures

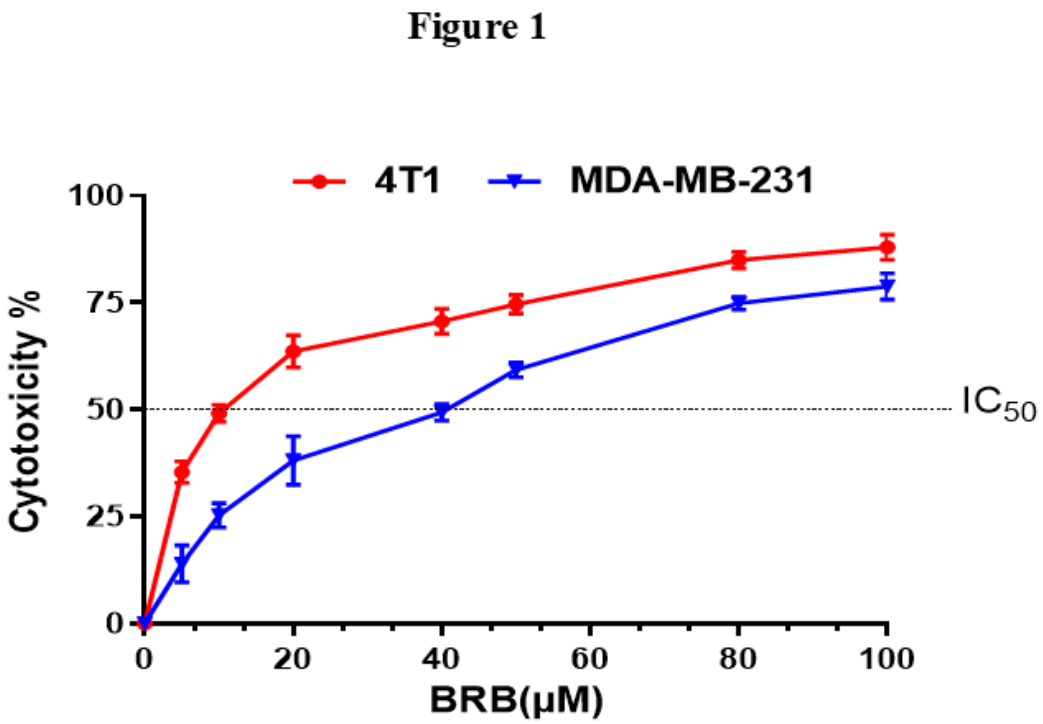

Figure 1

Cytotoxicity effects of berberine chloride (BRB) on human breast cancer cells MDA-MB-231(Blue line) and murine breast cancer cells 4T1 (Red line). After treatment of cells with increasing concentrations (0–100 μM) of BRB for 48 h, the percentage of cell cytotoxicity was determined using the crystal violet assay. The results are expressed as a mean percentage of control growth ± Standard Error of the Mean (SEM) of three independent experiments.

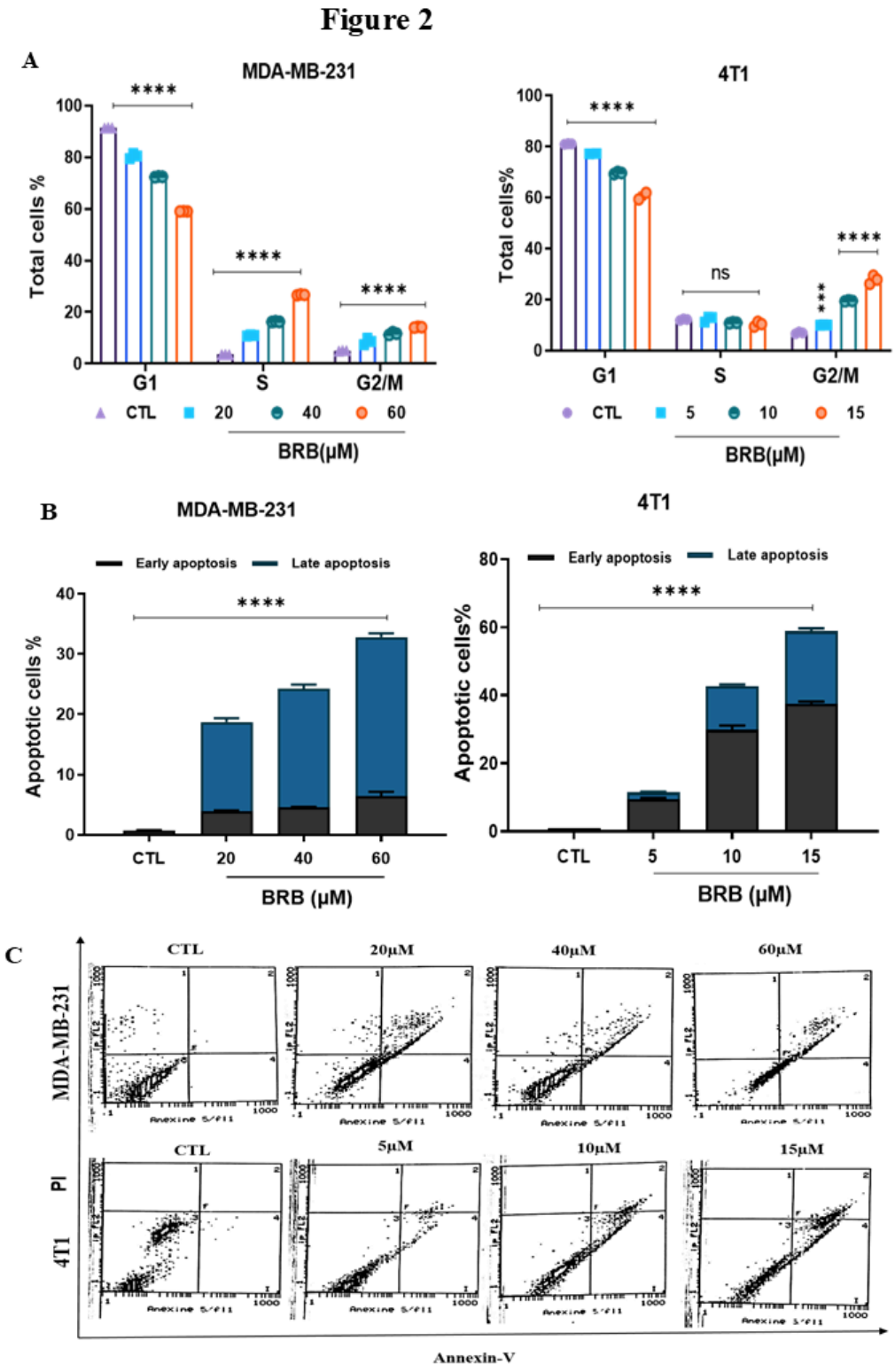

Figure 2

CellCycle Analysisand Apoptosisquantification followingBRB treatment. Cellcycle distribution in MDA-MB-231 and 4T1 cells was quantitatively assessed after48-hour exposureto decreasingBRB concentrations (A). Phase quantification revealeddistinct populations in Gap 1 (G1), DNA synthesis(S), and Gap 2/Mitosis(G2/M) phases. Representativeimages of apoptotic cells(B). Apoptotic response was evaluated through annexinV/propidium iodide (PI) dual staining. Early apoptotic cells were identifiedas annexinV^+/PI^-, while late apoptoticpopulations showed annexinV^+/PI^+ staining. BRB treatment demonstratedconcentration-dependentinduction of apoptosisin both cell lines after48 hours(C). Data represent mean± SEM from three independent

replicates. Statistical significance was determined using two-wayANOVA with Dunnett'smultiple comparisontest, showing highly significant effects(****p<0.0001) comparedto the untreatedcontrol (CTL).

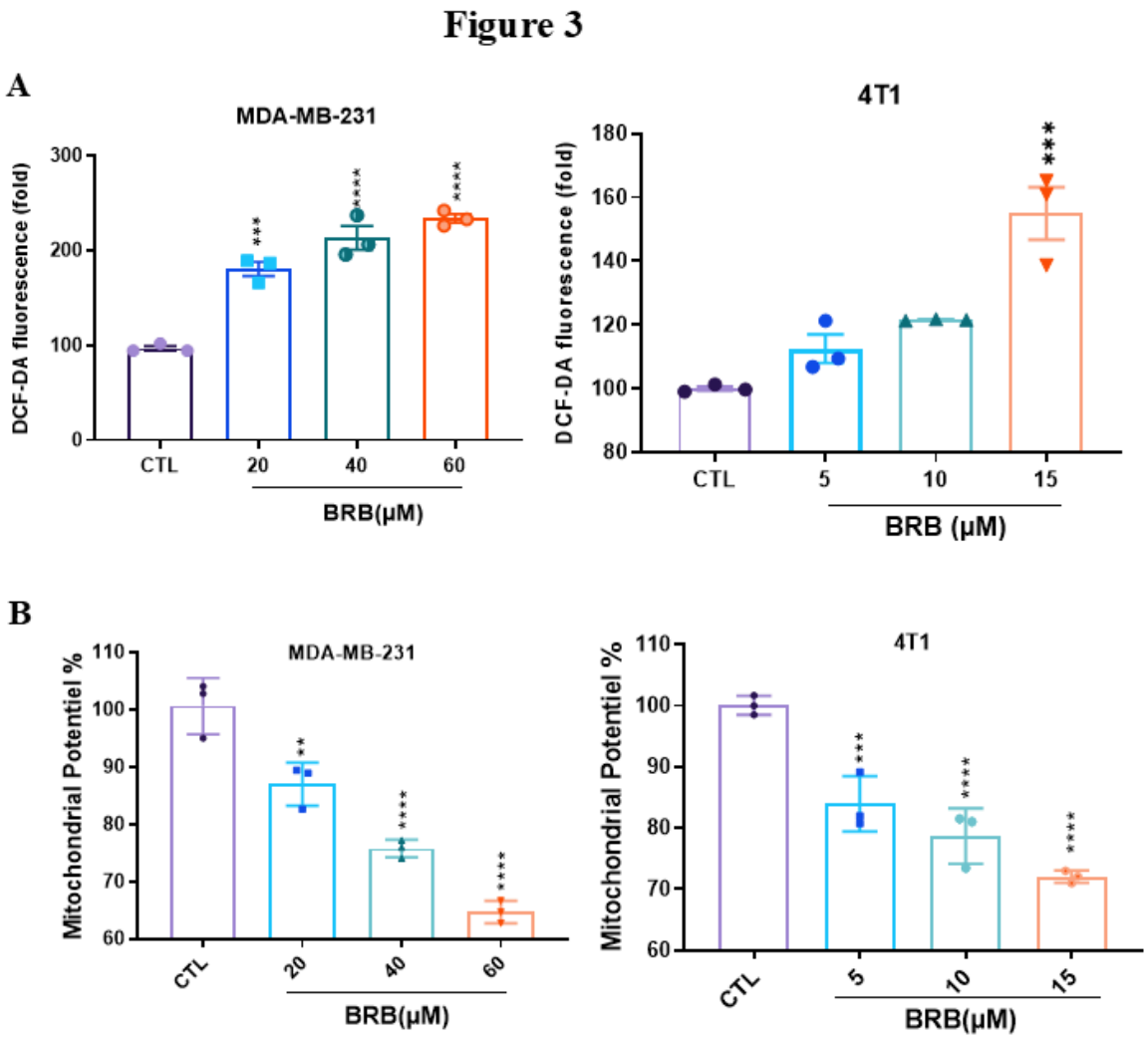

Figure 3

BRB induces reactive oxygen species (ROS) accumulation (A) and mitochondrial membrane potential (ΔΨm) loss (B) in MDA-MB-231 and 4T1 cell lines. Both cell lines were stained with DCFH or rhodamine 123 after 48 h of treatment with different concentrations of BRB. Data are expressed as mean ± Standard Error of the Mean (SEM) of three independent experiments; p-values were determined by a two-way ANOVA followed by Dunnett's multiple comparison test. **** p < 0.0001 compared to the control (CTL) group.

Figure 4

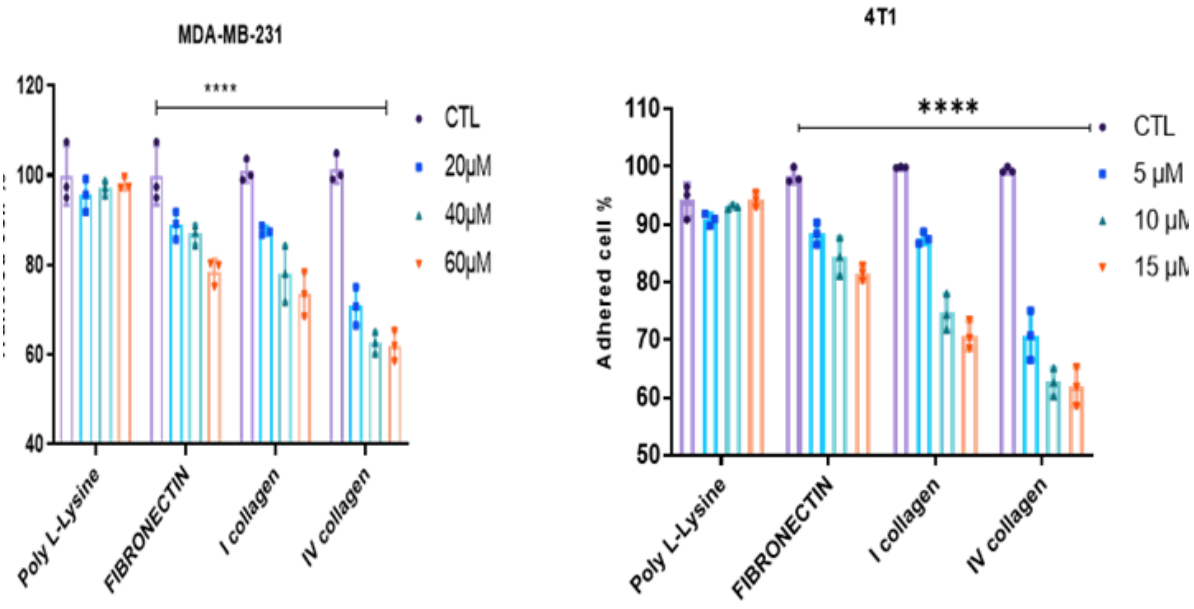

Figure 4

Effect of BBR on MDA-MB-231 and 4T1 cell adhesion. The cells were treated with increasing concentrations of BRB before being introduced into wells previously coated with various extracellular matrices (fibronectin, collagen I, collagen IV, and poly-L-lysine). Data are expressed as mean ± Standard Error of the Mean (SEM) of three independent experiments; p-values were determined by a two-way ANOVA followed by Dunnett's multiple comparison test. **** p< 0.0001 compared to the control (CTL) group.

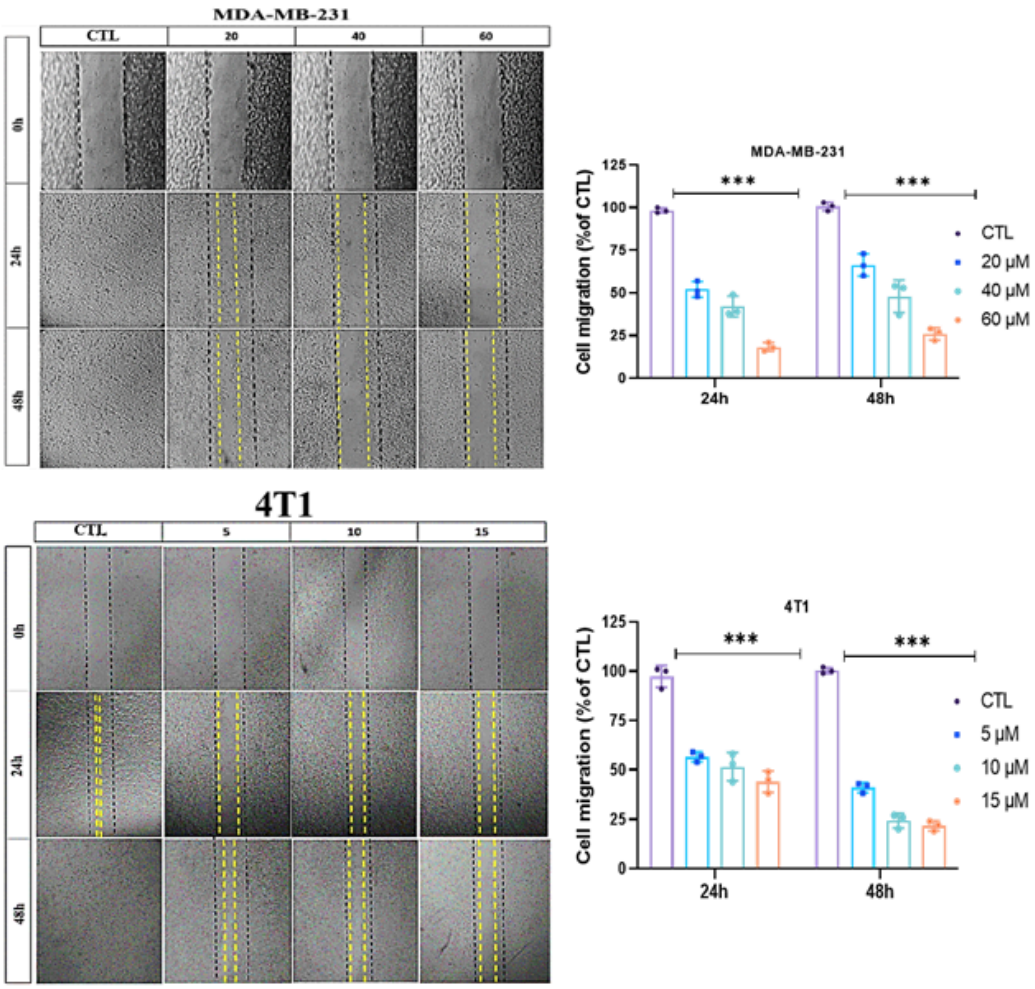

Figure 5

Effect of BBR on MDA-MB-231 and 4T1cell migration. (A)Representative images of wound healing assays for cells treated with various concentrations of BBR, for 0h, 24, and 48 h.(B) The percent recovery as determined in the scratch wound healing assay. Data are expressed as mean ± Standard Errorof the Mean(SEM) of three independent experiments; p-values were determinedby a two-way ANOVA followed by Dunnett's multiple comparison test. **** p< 0.0001 comparedto the control (CTL) group.

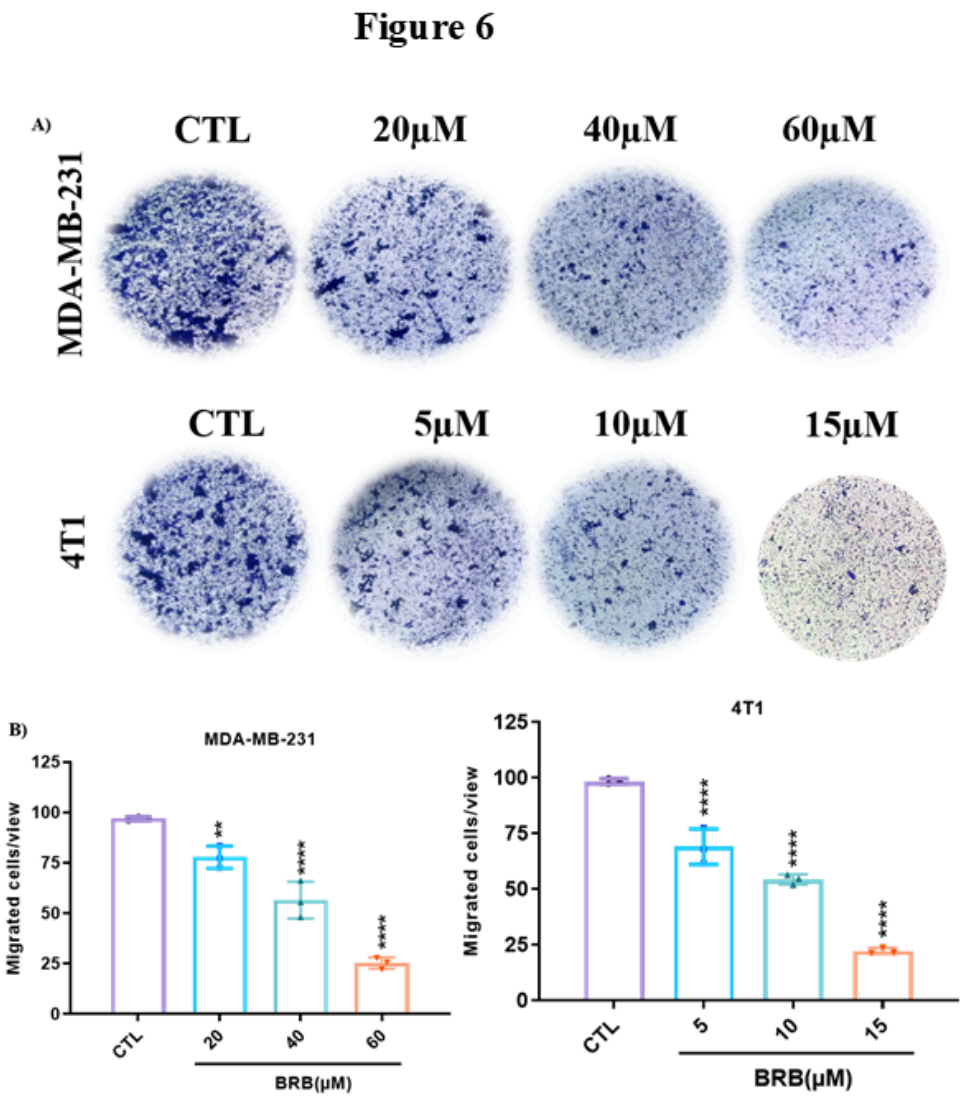

Figure 6

(A). Effect of BBR on MDA-MB-231 and 4T1cell migration. (B)Representative images of transwellassays for cells treated with various concentrations of BBR, for 48 h.(C). The percentage of migrated cells per view. Data are expressed as mean ± Standard Error of the Mean (SEM) of three independent experiments; p-values were determined by a two-way ANOVA followed by Dunnett's multiple comparison test. **** p< 0.0001

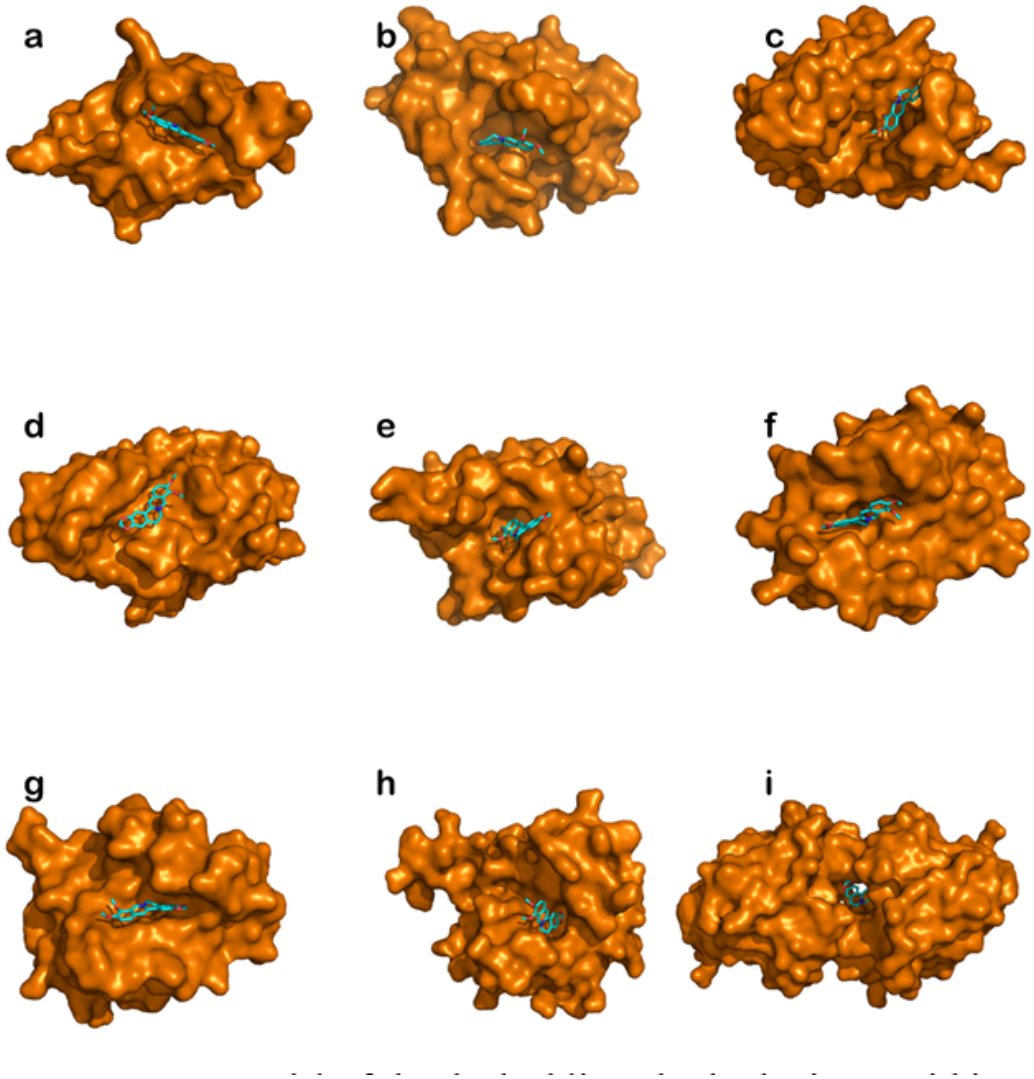

Figure 7

3D model of the docked ligand « berberine » within the binding cavity of the targeted receptors : MDM2-P53 (a), BCL2 (b), Caspase 3 (c), Caspase 8 (d), Caspase 9 (e), MCL1-BAX (f), MCL1-BID (g), MMP-2 (h) and MMP-9 (i).

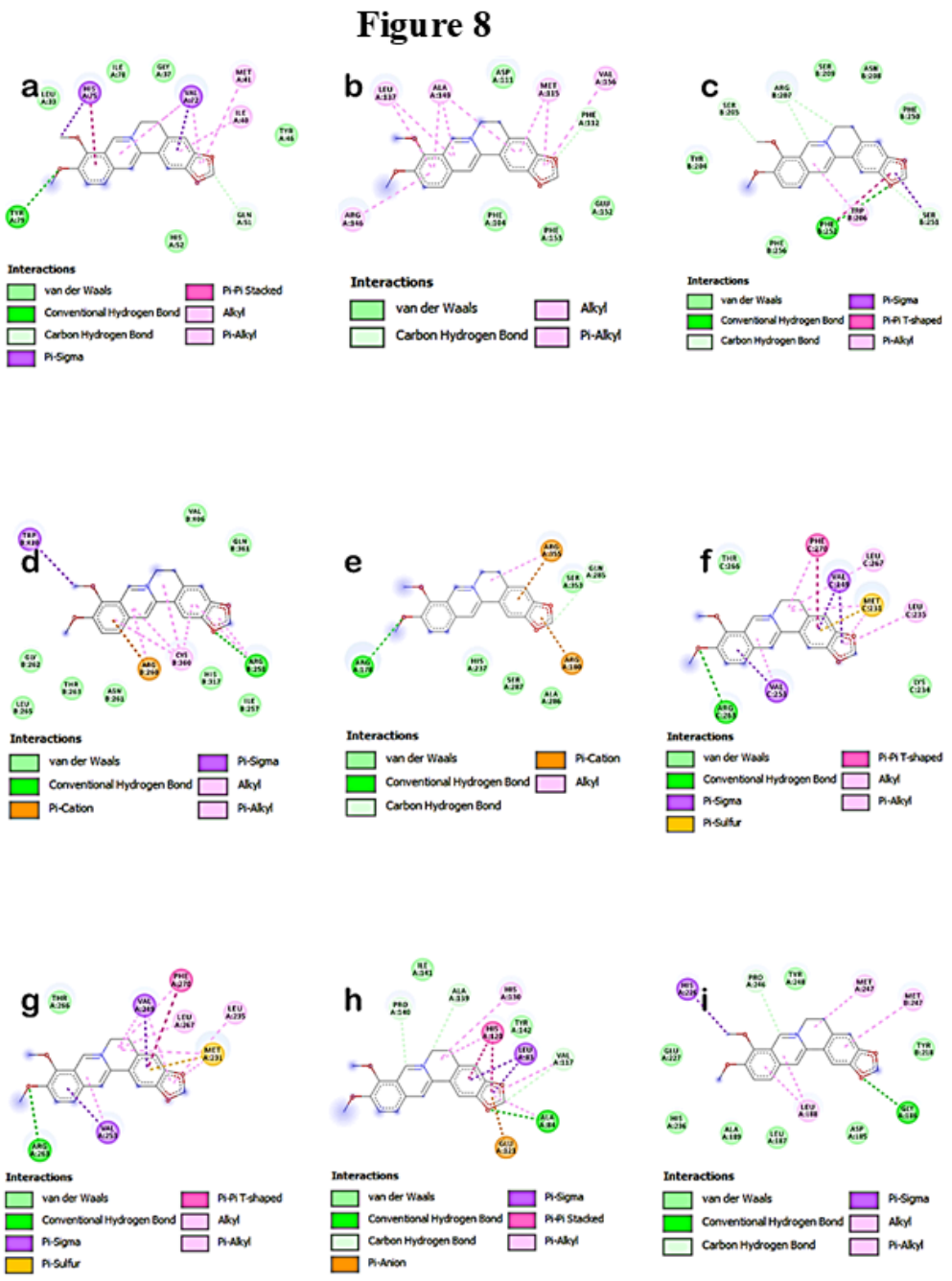

Figure 8

2D model of different interactions formed by the docked ligand « berberine » within the active site of the targeted receptors : MDM2-P53 (a), BCL2 (b), Caspase 3 (c), Caspase 8 (d), Caspase 9 (e), MCL1-BAX (f), MCL1-BID (g), MMP-2 (h) and MMP-9 (i).

Supplementary Files

This is a list of supplementary files associated with this preprint. Click to download.

- Slide1.png